Influence of diamond surface termination on Thermal Boundary Conductance between Al and diamond

Christian Monachon[1, a)] and Ludger Weber[1]

Laboratoire de Métallurgie Mécanique, Ecole Polytechnique Fédérale de Lausanne, Lausanne, Switzerland

The effect of diamond surface treatment on the Thermal Boundary Conductance (TBC) between Al and diamond is investigated. The treatments consist in either of the following: exposition to a plasma of pure Ar, Ar:H and Ar:O, and HNO_3:H_2SO_4 acid dip for various times. The surface of diamond after treatment is analyzed by XPS, revealing hydrogen termination for the as-received and Ar:H plasma treated samples, pure sp^2 termination for Ar treated ones and oxygen (keton-like) termination for the other treatments. At ambient, all the specific treatments improve the TBC between Al and Diamond from 23±2 $MWm^{-2}K^{-1}$ for the as-received to 65±5, 125±20, 150±20, 180±20 $MWm^{-2}K^{-1}$ for the ones treated by Ar:H plasma, acid, pure Ar plasma and Ar:O plasma with an evaporated Al layer on top, respectively. The effect of these treatments on temperature dependence are also observed and compared with the most common models available in the literature as well as experimental values in the same system. The results obtained show that the values measured for an Ar:O plasma treated diamond with Al sputtered on top stay consistently higher than the values existing in the literature over a temperature range from 78 to 290 K, probably due a lower sample surface roughness. Around ambient, the TBC values measured lay close to or even somewhat above the radiation limit, suggesting that inelastic or electronic processes may influence the transfer of heat at this metal/dielectric interface.

[a)]Corresponding author, email adress: christian.monachon@epfl.ch

I. INTRODUCTION

Interfaces and surfaces have a crucial influence on the functional properties of materials, e.g. chemical properties are strongly influenced by surface functionalization[1], passivation of an interface with a nm-sized layer in heterojunction solar cells paves the way to drastically higher photovoltaic conversion performances[2], and grain boundaries control the properties of the final device, *e.g.* in varistors[3]. In this respect, thermal properties are no exception and Thermal Boundary Conductance (TBC) between metals and dielectrics has been shown to depend quite strongly on the quality of that interface. Lyeo *et al.*[4] observed an effect of the surface termination with hydrogen of both diamond and silicon interfaces with lead and bismuth. In general, H termination leads to decreased TBC between metal and substrate. Hopkins *et al.*[5] observed that an oxide interlayer between Cr and Si increases TBC as compared to a Si/Cr clean interface due to the formation of a nanometer-sized silicide interlayer in the latter. On the other hand, the present authors have found that an Ar plasma treatment of an AlN substrate increases the TBC between Al and AlN due to the elimination of the native oxide layer on AlN[6]. Schmidt *et al.*[7] found that a 5 nm Ti interlayer between Al and graphite increases the TBC between these materials to the value of the Ti/graphite couple. Recently, Losego *et al.*[8] showed that the functionalization of a silicon dioxide surface with polymers can change substantially both the adhesion and the TBC with a gold layer. Collins *et al.*[9] found that oxygenation and hydrogenation of diamond change the TBC between Al and diamond, to higher values for the former and lower for the latter. Finally, Hopkins *et al.*[10] recently reproduced this result with graphene instead of diamond and observed the same trends as Collins *et al.*. In this paper, we extend the work by Collins *et al.*[9] and we present a thorough investigation of the effect of various surface treatments on the Al/diamond TBC. The treatments that we apply to the diamond surface consist

in the exposure to a plasma of pure argon, argon:hydrogen, or argon:oxygen, as well as a a mix of acids, along with the reference of an as-polished diamond. We then characterize the diamond surface by X-ray Photoelectron Spectroscopy (XPS) after these treatments, and we measure the conductance between Al and the prepared diamonds by Time Domain ThermoReflectance (TDTR).

II. EXPERIMENTAL

A. Sample preparation

Samples of Al layers were deposited by evaporation in an Alcatel EVA 600 e-beam evaporator. To observe the effect of the deposition technique, sputtering in a Balzers BAS 450 sputter deposition system was used as an alternative. The deposition speeds used were of 14 (evaporation) and 6 $Ås^{-1}$ (sputtering), measured by a quartz microbalance and later verified by SEM[11] along with deposition time measurement, respectively. Four types of substrates were used of which three were used as calibration samples for comparison with literature values. They consist in two <100> silicon wafers, one with 100 nm of thermal oxide, one HF-dipped to remove the native oxide before deposition, a $< 0001 >$ oriented sapphire, and diamond substrates with various surface treatments. All the diamonds used were monocrystals of size 3x3x1 mm with $< 100 >$ orientation polished using diamond suspensions with particle sizes decreasing from 6 to 1 μm. After polishing, the samples were rinsed with acetone, ethanol and finally isopropanol. This state will later be referred to as "As Received" (AR). The diamonds were then treated using 4 different treatments.

a. Hydrogen plasma treatment. The samples were treated in a Balzers BAI730D chamber, using a 95:5 Ar:H mixture at a pressure of 10^{-3} mbar. The recombination enthalpy of the atomic H was used to heat up our samples and the temperature was

monitored using thermocouples set in the vicinity of the diamond. Two diamonds were placed at 13 and 16 cm from the center of the plasma, reaching respective temperatures of 900±50 and 700±50°C for 2 hours.

b. Acid treatment. Samples were put in a boiling solution of 1:1 (by volume) HNO_3:H_2SO_4 (with respective concentrations of 63 and 98%) at 200°C. Though the exact composition of the bath may vary, this type of procedure is known to produce an oxidized surface on diamond[12–14]. Treatment times of 1, 5, 10, 30 and 60 min were used in order to observe any possible treatment time dependence on the interface thermal conductance.

c. Pure Ar plasma treatment. Samples were put in the same Balzers BAS 450 sputter deposition system as the one used for deposition, except that a RF source was used in RF etch mode, with no deposition target, creating a 500 W plasma with 3x10$^-$2 mbar Ar to etch the diamond surface. Two treatment times were used; 1 and 5 min. In the case of 5 min treatments, two separate identical treatments were applied. In one case, the Al layer was then directly sputtered onto the treated sample. In the other, 4 samples were etched and the sample subsequently exposed to clean room air. One sample was transferred to the Alcatel EVA 600 evaporator, 2 were kept for the XPS investigation, and one was put back in vacuum in the sputter deposition system.

d. Oxygen plasma treatment. Samples were treated in a Fischione model 1020 plasma cleaner. The Ar:O_2 ratio of the plasma is 3:1. Treatment times of 0.5, 1, 5, 10, 15 and 30 min were used on several diamonds in order to observe any eventual treatment time dependence. Additionally, a sample was plasma-treated for 10 min and rinsed with acetone, ethanol and isopropanol afterwards to track a possible effect of the rinsing of the AR state.

For each type of treatment 2 samples were kept for XPS investigation. The treatment times used for acid and oxygen plasma were of 10 and 15 min respectively. On the

other samples, an Al layer was deposited using the equipment described earlier. The precise thickness of the deposited layers was later verified by scanning electron microscopy[11] and picosecond ultrasonics[15].

B. Time Domain ThermoReflectance

The experimental setup used for the TDTR experiments is a coaxial two-tints pump/probe experiment[16] and has already been described in detail elsewhere[11]. This setup uses a Spectra Physics tsunami femtosecond laser working at a repetition rate of 80 MHz and 790 nm wavelength[16], the beam of which is split into two parts, the pump (used to heat the sample surface) and the probe (to measure the reflectivity of the sample surface), which are focused on the same spot at the sample's surface. The pump beam passes through a sharp long wave-pass filter set a 790 nm and the probe passes through a short wave-pass filter set at the same wavelength. The length of the pump's optical path can be varied by a delay stage, thereby enabling the creation of a delay between the arrival of the pump and probe on the sample surface from 0 to 4.02 ns. The pump beam is modulated with an electro-optic modulator at a frequency of 10.7 MHz. After passing through the same short wave-pass filter as earlier to further improve the signal to noise ratio, especially with regard to stray light from the pump, the probe signal is monitored using a fast photodiode. The resulting signal is passed through and band-pass electronic filter at 10.7 MHz, and is then amplified and fed to a Zurich Instrument Hf2Li lock-in amplifier. We calculate the X/Y ratio of the values measured by the lock-in, for it decreases the impact of a change in the overlap of the two spots[17]. We use spots of about 5 μm e^{-2} radius for both pump and probe, achieving fluences between 0.1 (78 K) and 0.6 mJcm^{-2} (298 K), leading to temperature rises of less than 0.1 K. Thus, correction of the metal lattice temperature due to high initial heating[18] in the thermal model is not necessary. Beam steering of

the pump is monitored using a CMOS camera in the beamline as described in[16] and is kept under 1 μm over the full range of time delays. We use the model first proposed by Cahill[17,19] to extract the values of TBC by fitting the model to the experimental data. The main fitting parameter is the thermal boundary conductance, but the diamond substrate conductivity has also to be allowed to vary to get a good fit. The value of this substrate conductivity at ambient temperature remains consistent for each individual diamond and is in the range typically admitted for industrial diamonds, *i.e.* 1000-1500 $Wm^{-1}K^{-1}$[20,21]. To rationalize the fact that we have to change the substrate conductivity, we calculate the sensitivities of the model used for data extraction to TBC and substrate conductivity k_{sub} as a function of delay time, using the data obtained for 177 nm Al sputtered on Ar:O treated diamond, using the formula:[17]:

$$S_{i(T)} = \frac{\partial ln\Big[-\frac{X(t,T)}{Y(t,T)}\Big]}{\partial lni(T)} \tag{1}$$

with i the parameter of interest. Figure 1 shows a contour plot obtained from equation 1. Among other things it shows that at low temperatures, below 180 K, $S_{ksubstrate}$ is much lower in magnitude than S_{TBC} and an increase in the former tends to flatten the obtained X/Y curve as a function of delay time, while an increase in the latter tends to make the curve steeper as a function of delay time. At intermediate temperatures, $S_{ksubstrate}$ becomes larger but has practically no impact on the slope of the curve as a function of time (it stays around 1 for the whole delay time range), while S_{TBC} becomes somewhat lower (actually down to 0 at long delay times), but the dependence of the slope of the X/Y curve as a function of time increases further (*e.g*) it passes from 1 to 0 over the whole delay time around 250 K). At temperatures higher than 270 K, a third region can be defined where $S_{ksubstrate}$ shows the same behavior as S_{TBC} at delay times higher than about 2.5 ns, thus increasing the slope of the curve, but at these delay times S_{TBC} is essentially zero and therefore

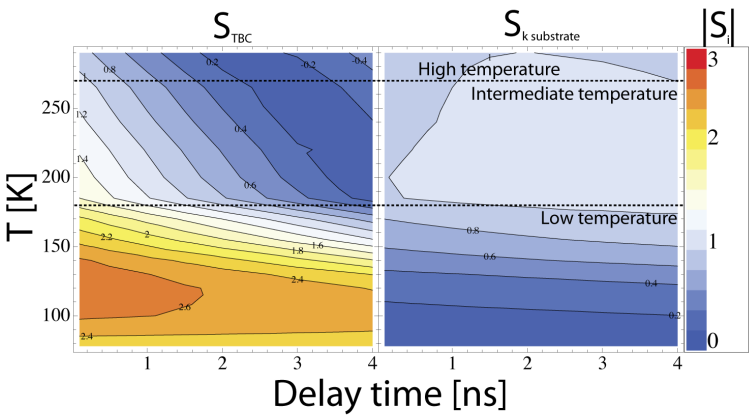

Figure 1. Sensitivities of our experiment to TBC (S_{TBC}) and to substrate conductivity $S_{ksubstrate}$ calculated according to equation 1 with the data recorded for a sample of 177 nm Al sputtered on an Ar:O plasma-treated diamond. Three main temperature regions can be distinguished for their behavior as a function of delay time.

this can be used to precisely fit $k_{substrate}$ first, and then delay times shorter than 2 ns and longer than 3 ns can be used to find the TBC. We therefore conclude that the method we use for data extraction can discern correctly between $k_{substrate}$ and TBC as parameters since the response of the model to a change in either of these parameters is substantially different, and thus that there is only one combination of $k_{substrate}$ and TBC that fits adequately the obtained curves. The thus obtained conductivity of the substrate is probably underestimated since the phonon mean free path in diamond is non-negligible compared to the spot size[22]. Indeed, heat emitted from a source smaller than the phonon mean free path of a material changes its perceived thermal conductivity as first pointed out theoretically by Chen[23] and later demonstrated experimentally by Siemens *et al.*[24]. For temperature-dependent measurements the samples were mounted into an optical cryostat fed with liquid

nitrogen, in which the temperature is measured using a silicon probe on the sample substrate.

C. X-ray Photoelectron spectroscopy

X-ray photoelectron spectroscopy (XPS) data were collected by an Axis Ultra (Kratos analytical, Manchester, UK) under ultra-high vacuum condition ($<10^{-8}$ Torr), using a monochromatic Al Kα X-ray source (1486.6 eV). The source power was maintained at 150 W (10 mA, 15kV). The emitted photoelectrons were sampled from a rectangular area of 750 by 350 μm. Gold (Au $4_f^{7/2}$) and copper (Cu $2_p^{3/2}$) lines at 84.0 and 932.6 eV, respectively, were used for calibration. To compensate for any charging effects, the main carbon peak was calibrated at 285.5 eV, a value measured on conductive diamond containing nitrogen[25–27]. The carbon peak and its sub peaks were studied since quantifying the oxygen can be deluding due to physisorbed water molecules or inorganic dusts that can influence the quantitative elemental analysis on the diamond surface.

III. RESULTS

A. Calibration

Figure 2 shows the results obtained in the calibration step of our system. Over 4 measurements, we found an Al/Sapphire TBC of 190±20 $\mathrm{MWm^{-2}K^{-1}}$, which is within error equal to to the result of 185 $\mathrm{MWm^{-2}K^{-1}}$ from Hopkins *et al.*[28] and Stoner *et al.*[29] as well as the 200 $\mathrm{MWm^{-2}K^{-1}}$ of Stevens *et al.*[30]. The conductivity value found for SiO_2 of 1.27±0.1$\mathrm{Wm^{-1}K^{-1}}$ is the same as that found by Costescu *et al.*[17]. Finally, our value over 4 measurements for Al on HF-dipped Si is 350 ±

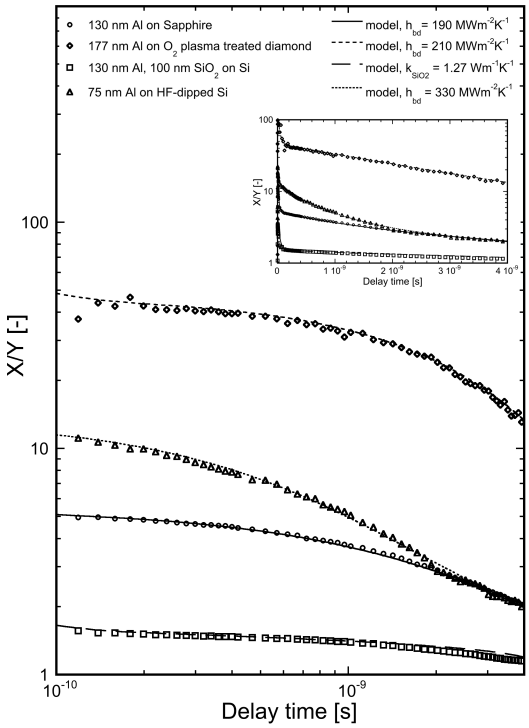

Figure 2. Calibration tests of our equipment for three samples: 130 nm Al evaporated on Sapphire (circles) and simulation used for TBC extraction (continuous line), 130 nm Al evaporated on 100 nm thermal SiO_2 on silicon (squares) and simulation (long dashed line), 177 nm Al sputtered on Ar:O_2 plasma-treated diamond (diamonds, for comparison with calibration samples) and simulation (dashed line), 75 nm Al evaporated on HF-dipped Si (triangles) and simulation (dotted line). The spot size had an average diameter of 4.7 μm in every cases. The thermophysical data not mentioned in the figure are k_{Al}=237 $Wm^{-1}K^{-1}$, $C_{v,Al}$=2.44 $MJm^{-3}K^{-1}$, $k_{Al_2O_3}$=30 $Wm^{-1}K^{-1}$, C_{v,Al_2O_3}=3 $MJm^{-3}K^{-1}$, k_{Si}=142 $Wm^{-1}K^{-1}$, $C_{v,Si}$=1.64 $MJm^{-3}K^{-1}$, C_{v,SiO_2}=1.62 $MJm^{-3}K^{-1}$, k_C=1400 $Wm^{-1}K^{-1}$, $C_{v,C}$=1.83 $MJm^{-3}K^{-1}$.

20 $MWm^{-2}K^{-1}$, in full agreement with the value of 350 $MWm^{-2}K^{-1}$ reported by

Minnich *et al.*[22].

B. Substrate conductivity

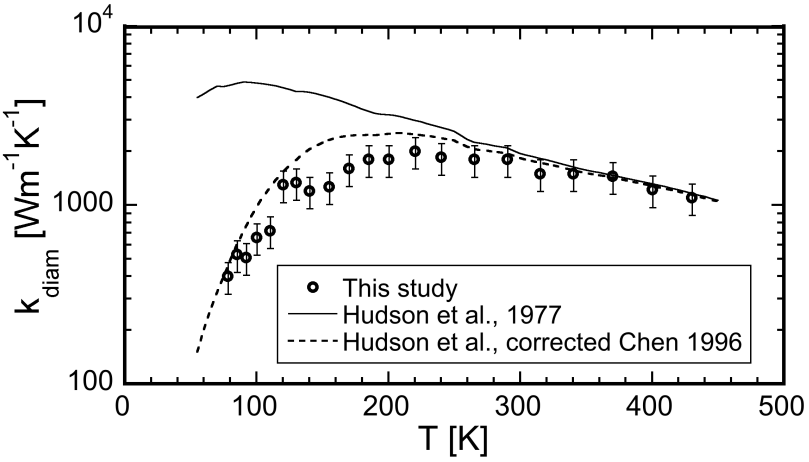

Figure 3. Measured diamond thermal conductivity, compared to values from Hudson *et al.*[31] and these values corrected for a laser spot size of 4.7 μm[22,23].

Figure 3 shows the results obtained for the conductivity of an Ar:O plasma-treated diamond with a 177 nm Al layer sputtered on it, compared with literature values from Hudson *et al.*[31] and the same values with a correction due to a 4.7 μm spot size proposed by Chen[23].

C. Influence of surface treatment

The TBC values found as a function of both the diamond surface treatment and the Al layer deposition technique are given in table I. The *rms* roughness of all the substrates investigated was measured using a Focused Ion Beam to be less than 2 nm.

Table I. Measured TBCs as a function of the diamond surface treatment and Al deposition technique. A typical standard deviation over 4 measurements is given after the values.

Surface treatment	Al layer deposition technique	Measured TBC [$MWm^{-2}K^{-1}$]
As received	evaporated	23±2
As received	sputtered	23±2
Ar:H plasma treated, 700°C	evaporated	54±5
Ar:H plasma treated, 900°C	evaporated	65±5
Acid treated, 1 min	evaporated	95±15
Acid treated, 10-60 min	evaporated	125±20
Acid treated, 10 min	sputtered	165±20
Ar RF plasma etched, 1-5 min	sputtered	205±20
Ar RF plasma etched, 5 min, air exposed	sputtered	180±20
Ar RF plasma etched, 5 min, air exposed	evaporated	150±15
Ar:O plasma treated, 30s-30 min	evaporated	180±20
Ar:O plasma treated, 15 min, rinsed afterwards	evaporated	105±20
Ar:O plasma treated, 15 min	sputtered	230±25

D. XPS analysis

XPS spectra were taken on diamonds with each surface treatment (2 diamonds in each case). Only O and C peaks were found on all samples, except for the H plasma-treated and Ar plasma treated ones, where traces of Al and Si and Al were respectively found. Quantification of the C_s^1 subpeaks was performed using the casaXPS software using gaussian-lorentzian curves, varying the height of the curves as needed

and their full width at half maximum (FWHM) between 0.8 and 1.8 eV. Five sub peaks were identified in the carbon peak. The main peak at 285.5 eV is taken to be sp^3 carbon. Three peaks were identified at higher energies; one at 286.2 eV, attributed to C-O surface termination[27,32], one at 286.7, attributed to C-H surface termination[25,26,34,35], and one above 288 eV, attributed to C=O bonds. This last peak disappeared once the sample had been subjected to a bakeout at 300°C for 10 min, thus we attribute it to surface contaminations. Moreover, we concentrate on C-O bonds since they have been observed to be more stable at low temperatures[36–38]. One peak is identified at lower energies than the main peak, at 284.4 eV and is attributed to sp^2 surface termination[27,32,34,35]. This peak was found to be shifted to 284.0 eV for the case of the Ar:O plasma treated samples.

Figure 4 shows the recorded XPS signal around the C_s^1 peak of diamond as a function of sample surface treatment (a) and an example of quantification using gaussian-lorentzian fits (b).

Table II shows the proportions of the C_s^1 subpeaks derived from the recorded XPS signals at the binding energies fixed as presented earlier in the text.

Table II. Proportions of the C_s^1 subpeaks in the recorded XPS signals. Two measurements were taken in each case on 2 different diamonds.

	Bonding type proportion [%]			
Treatment	C sp^3	C sp^2	C-O	C-H
As received	91.3±2.1	3.9±2.3	<0.1	4.8 ± 0.2
Ar:H plasma treated	87.2±6.8	4.3±1.0	<0.1	6.2±2.5
HNO_3:H_2SO_4 at 200°C	85.7±3.1	7.5±3.0	6.2±0.1	0.6±0.1
Ar plasma etched	55±0.2	42±0.2	0.6±0.3	0.4±0.3
Ar:O plasma treated	81.9±1.4	6.6±0.5	11.4±1.9	<0.1

E. Temperature dependence of TBC

Temperature-dependent measurements were performed on the 2 samples exhibiting the most extreme TBC while being of known surface composition (*i.e.* without the as received samples), one consisting of an Ar:O plasma-treated diamond with a 177 nm Al layer sputtered on it and the other consisting of an 700°C Ar:H plasma treated diamond with a 85 nm Al layer evaporated on it. Figure 5 shows the results obtained. As a guide to the eye the Maximum Transmission Limit, the Radiation Limit as well as the Diffuse and Acoustic Mismatch Models have been plotted in the approximation of a Debye solid using values for speeds of sound and Debye temperatures from Swartz and Pohl[39]. This second limit and the two models are based on the same equation:

$$TBC = \frac{1}{2}\sum_{p}\int_{0}^{\frac{\pi}{2}}\int_{0}^{\omega_{max}} \hbar\omega v_p \frac{\partial n_{\omega,p,T}}{\partial T}\frac{\omega^2}{2\pi^2 v_p^3}\alpha_{1\to 2}(\theta,p,\omega)cos\theta sin\theta d\theta d\omega \qquad (2)$$

with p the polarization, θ the angle of incidence of a given phonon, ω its angular frequency, T the temperature, v the speed of sound and $\alpha_{1\to 2}$ a coefficient of transmission. $n(\omega,T) = \frac{1}{e^{\frac{\hbar\omega}{k_B T}}-1}$ is the Planck distribution function. The maximum angular frequency ω_{max} is taken to be $\theta_{D,1}k_B\hbar^{-1}$ with $\theta_{D,1}$ the lower of the Debye temperatures of the solids on either side of the interface (solid 1 in our formulation of the problem). $\alpha_{1\to 2}$ is the parameter that changes according to the model (or limit) used.

For the Acoustic Mismatch Model, it takes the form[39,40]:

$$\alpha_{1\to 2} = \frac{4\frac{\rho_2 c_{p,2}}{\rho_1 c_{p,1}}\frac{cos\theta_{p,2}}{cos\theta_{p,1}}}{\left(\frac{\rho_2 c_{p,2}}{\rho_1 c_{p,1}} + \frac{cos\theta_{p,2}}{cos\theta_{p,1}}\right)^2} \qquad (3)$$

and the upper limit of the integral on θ in equation (2) is changed to $\theta_{p,1}^{crit} = sin^{-1}(\frac{v_{p,1}}{v_{p,2}})$. For the Diffuse Mismatch, the form is different[39]:

$$\alpha_{1\to2}(\omega) = \alpha_{1\to2} = \frac{\sum_p v_2^{-2}(p)}{\sum_p v_1^{-2}(p) + \sum_p v_2^{-2}(p)} \tag{4}$$

For the radiation limit, the transmission coefficient from the solid with the higher θ_D to the one with the lower, $\alpha_{2\to1}$, is taken to be to be 1. This leads to[39]:

$$TBC = \frac{1}{8\pi^2}\sum_p \int_0^{\omega_{max,1}} \hbar\omega^3 v_{p,2}^{-2} \frac{\partial n_{\omega,p,T}}{\partial T} d\omega \tag{5}$$

IV. DISCUSSION

The accurate restitutions of literature values by our setup (figure 2) suggests that it is adequate for TDTR measurements.

A. Substrate conductivity

To validate our hypothesis of an effect of spot size S on the measured substrate conductivity k_{eff} we use conductivity values for diamond Ib from Hudson *et al.*[31]. We calculate the corresponding mean free path Λ in the diamond using the gas kinetics formula:

$$\Lambda = \frac{3k}{C_v v} \tag{6}$$

with k the thermal conductivity, C_v the volumetric heat capacity and v the geometrical average of the sound velocities in diamond. We correct these conductivity values using the simplified formula proposed by Chen[23]:

$$k_{corr} = \frac{\frac{3S}{4\Lambda}}{\frac{3S}{4\Lambda} + 1} k_{Diamond} \tag{7}$$

Figure 3 suggests that the choice of substrate conductivity as an additional free parameter is justified as the measured conductivities are close both in trend and

magnitude to the one predicted by equation 7. The discrepancies with the values from Hudson *et al.* can be rationalized by three ways: 1) the conductivity of the diamond can vary significantly with its nitrogen content[41], an effect that is expected to be larger at lower temperatures, explaining the lower values found, 2) we assume a linear dispersion relation and a mean free path that is not dependent on the phonon wavelength which is a crude[22?] yet commonly used approximation and 3) the sputter deposition method used in this case may implant Ar atoms in the lattice, also decreasing $k_{substrate}$. Thus, in accordance with Minnich *et al.*[22] our results tend to show that a size-limited heat source affects the measured conductivity of the substrate material. These results agree with those of Siemens *et al.*[24], since they invoke the same physical phenomenon to model the influence of the heat source size, though in their contribution the decrease in measured thermal conductivity is accounted for using an additional interface thermal resistance term instead of a change in substrate conductivity.

B. Effect of surface treatments

Table I shows that all the treatments applied to the diamond substrates investigated increased the TBC as compared to the as-received state. Except for the acid dip, which shows a TBC of 95 ± 15 $MWm^{-2}K^{-1}$ after 1 min and stabilizes at 125 ± 20 $MWm^{-2}K^{-1}$ after 10 and more minutes, none of the applied treatments showed a time dependence measurable on TBC. Three factors can contribute to the improvement in TBC: cleanliness of the substrate, surface termination of the diamond surface, and roughness. The cleanliness of the substrate is shown to play a role in the as-received state since a rinsing with organic solvents decreases the TBC of an Ar:O plasma-treated diamond by a factor of 1.9. This decrease is taken to come from organic residues left after the rinsing, which decrease the adhesion between

layer and substrate[8,43]. We explain the lower conductance at the interface in the as-received state with this effect. The surface termination of the substrate seems to play a critical role as well. Treatment with a hydrogen plasma cleans the substrate but induces only a moderate increase in TBC as compared to the other three treatments. The fact that our value for H plasma treated diamond is higher than that of Collins *et al.* may be due to traces of Al and Si coming from the machine used, or to the lower roughness of our substrates[44,45]. The roughness would also explain why the sample treated at 900°C has a higher TBC than the one at 700°C since hydrogen treatment has been shown to smoothen $< 100 >$ faces of diamond[46,47]. The other 3 treatments increase significantly the TBC, up to 230±20 $MWm^{-2}K^{-1}$ for an Ar:O plasma treated diamond with a sputtered Al layer. This seems to be linked positively to a C-O surface termination, though it could also be due to the absence of surface hydrogen since pure Ar plasma treatments lead to similar values. The TBC increases when the proportion of this type of bond increases as observed in the difference between acid and plasma-treated samples. This result confirms the tendency reported by Collins *et al.*[9], though with absolute values higher by a factor of 2. This might be owed to the use of different ways of oxidizing the surface since acid and plasma treatment was used, not heating in an oxygen-rich atmosphere[48]. It could also be due to a difference in substrate roughness: Collins reports a roughness of 20 nm and such a roughness was shown to reduce the TBC in an Al/Si system by a factor of 2 as compared to a roughness of 0.6 nm and less[44,45]. Direct comparison of XPS spectra would be necessary to know if the first hypothesis has a significant impact or if the difference is only related to roughness. Table II suggests that unlike the Ar:O treated sample, C-H termination is still present on the acid treated sample, and that the quantity of C-O bonds measurable is 1.8 times higher in the former compared to the latter. The only other noticeable difference between the XPS results from Ar:O and acid-treated samples is the shift in sp^2 peak, for which we do not

have any explanation for the time being. The proportion of sp^2 bonds is also higher in these two samples than in the case of as-received and Ar:H-treated samples, which themselves show no significant difference. This proportion is even larger in the Ar etched samples which exhibit a very high TBC of 205±20 $MWm^{-2}K^{-1}$. This value drops significantly when the surface is exposed to air, meaning that the surface obtained is not stable, which also explains the lower value obtained for the evaporated Al layer on Ar etched substrate as compared to Ar:O treated substrate.

C. Influence of deposition technique

The technique used to deposit the Al layer has an influence on the measured TBC value in all cases but the As Received one. It is always higher in the case of sputtered layers, leading to an increase by a factor of 1.32, 1.2 and 1.13 for Acid, Ar plasma etched and Ar:O plasma treated samples respectively. We attribute this to an improved layer adhesion due to Ar ion bombardment during sputtering. This effect is not observed in the case of as-received sample since this bombardment also creates higher stresses in the film, leading possibly to delamination. Such delamination was indeed observed by SEM as blisters similar to the ones reported in a previous study[11] were present in the films deposited on AR substrates.

D. Temperature dependence

The temperature dependence observed on our samples follows the same trends as those previously reported[9,29], though our result for Ar:O treated samples show substantially higher values throughout the whole temperature range. Our results on Ar:H plasma treated diamond compare well with those of Stoner and Maris[29]

except at low temperature. This difference could come from the values used for the heat capacity and, especially, conductivity of the diamond as the latter depends significantly on the level of nitrogen impurities in the diamond used. The results on Ar:O treated diamonds seem to agree with the AMM at low temperature and progressively reach the DMM and finally the radiation limit, which suggest a behavior dominated by long-wavelength phonons at low temperature, with short-wavelength phonons capable of scattering on the interface roughness gradually appearing with increasing temperature. Finally, at ambient the models fail, probably because other processes become dominant. The fact that the radiation limit is attained and even exceeded suggests that processes involving either electrons[49] or phonons with higher energies[33,50] than the maximum energy in Al could take place, though the comparison with the Maximum Transmission Model[33] suggests that only a few inelastic processes occur. More work and experiments at higher temperature are necessary to develop a meaningful insight to the problem.

V. CONCLUSION

The Thermal Boundary Conductance between aluminum and diamond has been measured as a function of the surface preparation of the diamond and the deposition technique of the Al layer. The technique used to measure the TBC was Time Domain ThermoReflectance, which was shown to be sensitive both to TBC and diamond substrate conductivities. The values of these conductivities were shown to be underestimated by our measurements due to the use of a very small laser spot size in the measurements. The treatments used and compared with the as-received state were Ar:H plasma for 2 hours at 700 and 900°C, HNO_3:H_2SO_4 at 200°C, Ar RF etch plasma and Ar:O plasma for various times. The as-received and Ar:H plasma treated samples yielded substantially lower conductances than both acid treated and Ar:O

plasma treated samples. These two treatments seem to improve the TBC between Al and diamond by terminating the surface with oxygen atoms, which confirms previous results from literature, though pure sp^2 termination leads to very close results, suggesting that the absence of hydrogen on the surface matters most. The values obtained are however higher by a factor of 2 as compared to literature, which may be a roughness effect, or could otherwise be rationalized by a higher oxygen coverage with the treatment applied. The result is independent of the treatment duration after 30 s (Ar:O), 1 min (Ar RF etch) and 10 min (acids). The layer deposition technique is shown to have a direct influence on the measured TBC between Al and diamond, as the sputtered Al samples lead to consistently higher TBCs in all cases except in the as received condition, in which case a weak adhesion between layer and substrate – that is shown to decrease TBC – was observed. The TBC obtained at ambient with the Ar:O plasma treated diamond lay very close to –even slightly above– the radiation limit of the metal/dielectric couple, meaning that the two main models developed to assess TBC fall well below the values obtained, which is yet another call for an improved theoretical understanding of thermal transport through interfaces.

VI. ACKNOWLEDGMENTS

Financial support of C. Monachon by the SNSF Project No. 200021-121881 and 200020-135132 is gratefully acknowledged. The authors kindly acknowledge Christof Hollenstein and Loïc Curchod for their time and advice as well as the Ar:H plasma treatments, Nicolas Xanthopoulos (CIME, EPFL) for XPS measurements. Finally, Professor Hubert Girault of the Laboratoire d'Électrochimie Physique et Analytique (LEPA) at EPFL is acknowledged for providing the laser source for the experiments. Prof David G. Cahill of the University of Illinois at Urbana Champaign is gratefully

acknowledged for helpful discussions.

BIBLIOGRAPHY

[1]S. F. Bent, Surf. Science **500**, 879 (2002)

[2]S. Olibet, E. Vallat-Sauvain, and C. Ballif, Phys. Rev. B **76**, 035326 1 (2007)

[3]T. K. Gupta, J. Am. Ceram. Soc. **73**, 1817 (1990)

[4]H.-K. Lyeo and D. G. Cahill, Phys. Rev. B **73**, 144301 1 (2006)

[5]P. E. Hopkins, P. M. Norris, R. J. Stevens, T. E. Beechem, and S. Graham, J. Heat Transf **130**, 062402 1 (2008)

[6]C. Monachon, M. Hojeij, and L. Weber, Appl. Phys. Lett. **98**, 091905 1 (2011)

[7]A. J. Schmidt, K. C. Collins, A. J. Minnich, and G. Chen, J. Appl. Phys. **107**, 104907 1 (2010)

[8]M. D. Losego, M. E. Grady, N. R. Sottos, D. G. Cahill, and P. V. Braun, Nature Mater. Lett. **11**, 502 (2012)

[9]K. C. Collins, S. Chen, and G. Chen, Appl. Phys. Lett. **97**, 083102 1 (2010)

[10]P. E. Hopkins, M. Baraket, E. V. Barnat, T. E. Beechem, S. P. Kearney, J. C. Duda, J. T. Robinson, and S. G. Walton, Nano Let. **12**, 590 (2012)

[11]C. Monachon and Ludger Weber, Emerging Mat. Res. **1**, 89 (2012)

[12]P. W. May, J. C. Stone, M. N. R. Ashfold, K. R. Hallam, W. N. Wang, and N. A. Fox, Diam. Relat. Mater. **7**, 671 (1998)

[13]S. Kumaragurubaran, T. Yamada, and S. Shikata, Diam. Relat. Mater. **17**, 472 (2008)

[14]H. Kawarada, Surf. Sci. Rep. **26**, 205 (1996)

[15]C. Thomsen, H. T. Grahn, H. J. Maris, and J. Tauc, Phys. Rev. B **34**, 4129 (1986)

[16]K. Kang, Y. K. Koh, C. Chiritescu, X. Zheng, and D. G. Cahill, Rev. Sci. Instr. **79**, 114901 1 (2008)

[17]R. M. Costescu, M. A. Wall, and D. G. Cahill, Phys. Rev. B. **67**, 054302 1 (2003)

[18]F. Banfi, V. Juvé, D. Nardi, S. Dal Conte, C. Giannetti, G. Ferrini, N. Del Fatti and F. Vallée, Appl. Phys. Lett. **100**, 011902 1 (2012)

[19]D. G. Cahill, Rev. Sci. Instr. **75**, 5119 (2004)

[20]R. Tavangar, J. M. Molina, and L. Weber, Scripta Mat. **56**, 357 (2007)

[21]j.-F. Silvain, A. Veillere, J.-M. Heintz, C. Vincent, T. Guillemet, G. Lacombe, Y. Lu, and N. Chandra, Emerging Mat. Res. **1**, 75 (2012)

[22]A. J. Minnich, J. A. Johnson, A. J. Schmidt, K. Esfarjani, M. S. Dresselhaus, K. A. Nelson, and G. Chen, Phys. Rev. Let. **107**, 095901 1 (2011)

[23]G. Chen, J. Heat Transf. **118**, 539 (1996)

[24]M. E. Siemens, Q. Li, R. Yang, K. A. Nelson, E. H. Anderson, M. M. Murnane and H. C. Kapteyn, Nat. Mater. **9**, 26 (2010)

[25]L. Diederich, O. M. Kuettel, P. Ruffieux, T. Pillo, P. Aebi, and L. Schlapbach, Surf Sci. **417**, 41 (1998)

[26]L. Diederich, O. M. Kuettel, P. Aebi, and L. Schlapbach, Surf Sci. **418**, 219 (1998)

[27]P. Mérel, M. Tabbal, M. Chaker, S. Moisa, and J. Margot, Appl. Surf. Sci. **136**, 105 (1998)

[28]P. E. Hopkins, P. M. Norris, and R. J. Stevens, J. Heat Transf **130**, 022401 1 (2008)

[29]R. J. Stoner and H. J. Maris, Phys. Rev. B, **48**, 16373 (1993)

[30]R. J. Stevens, A. N. Smith, and P. M. Norris, J. Heat Transf **127**, 315 (2005)

[31]P. R. W. Hudson and P. P. Phakey, Nature **269** 15 227 (1977)

[32]J. J. B. Wilson, J. S. Walton, and G. Beamson, J. Electron Spectrosc. **121**, 183 (2001)

[33]C. Dames and G. Chen, J. Appl. Phys. **95**, 682 (2004)

[34]R. Graupner, J. Ristein, and L. Ley, Surf. Sci. **320**, 201 (1994)

[35]G. Francz, P. Kania, G. Gantner, H Stupp, and P. Oelhafen, Physica Status Solidi A **154**, 91 (1996)

[36]P. E. Pehrsson and T. W. Mercer, Surf Sci. **460**, 74 (2000)

[37]H. Tamura, H. Zhou, K. Sugisako, Y. Yokoi, S. Takami, M. Kudo, K. Teraishi, A. Miyamoto, A. Imamura, M. N.-Gamo, and T. Ando, Phys. Rev. B **61**, 11025 (2000)

[38]H. Yang, L. Xu, C. Gu, and S. B. Zhang, Appl. Surf. Sci. **253**, 4260 (2007)

[39]E. T. Swartz and R. O. Pohl, Rev. Mod. Phys. **61**, 605 (1989)

[40]W. A. Little, Can. J. Phys. **37**, 334 (1959)

[41]Y. Yamamoto, T. Imai, K. Tanabe, T. Tsuno, Y. Kamazawa and N. Fujimori, Diam. Relat. Mater. **6**, 1057 (1997)

[42]K. Esfarjani, Gang Chen and H. T. Stokes, Phys. Rev. B **84**, 085204 1 (2011)

[43]G. Tas, R. J. Stoner, H. J. Maris, G. W. Rubloff, G. S. Oehrlein, and J. M. Halbout, Appl. Phys. Let. **61**, 1787 (1992)

[44]P. E. Hopkins, L. M. Phinney, J. R. Serrano and T. E Beechem, Phys. Rev. B **82** 085307 (2010)

[45]J. C. Duda and P. E. Hopkins, Appl. Phys. Lett. **100** 111602 (2012)

[46]O. M. Kuettel, L. Diederich, E. Schaller, O. Carnal and L. Schlapbach, Surf. Sci. **337**, 812 (1995)

[47]P. John and M. D. Stoikou, Phys. Chem. **13**, 11503 (2011)

[48]H. Gamo, K. Iwasaki, K. Nakagawa, T. Ando, and M. N. Gamo, J. Phys Conf. Ser. **61**, 332 (2007)

[49]G. D. Mahan, Phys. Rev. B **79**, 075408 1 (2009)

[50]P. E. Hopkins, J. C. Duda, and P. M. Norris, J. Heat. Transf. **133**, 062401 1 (2011)

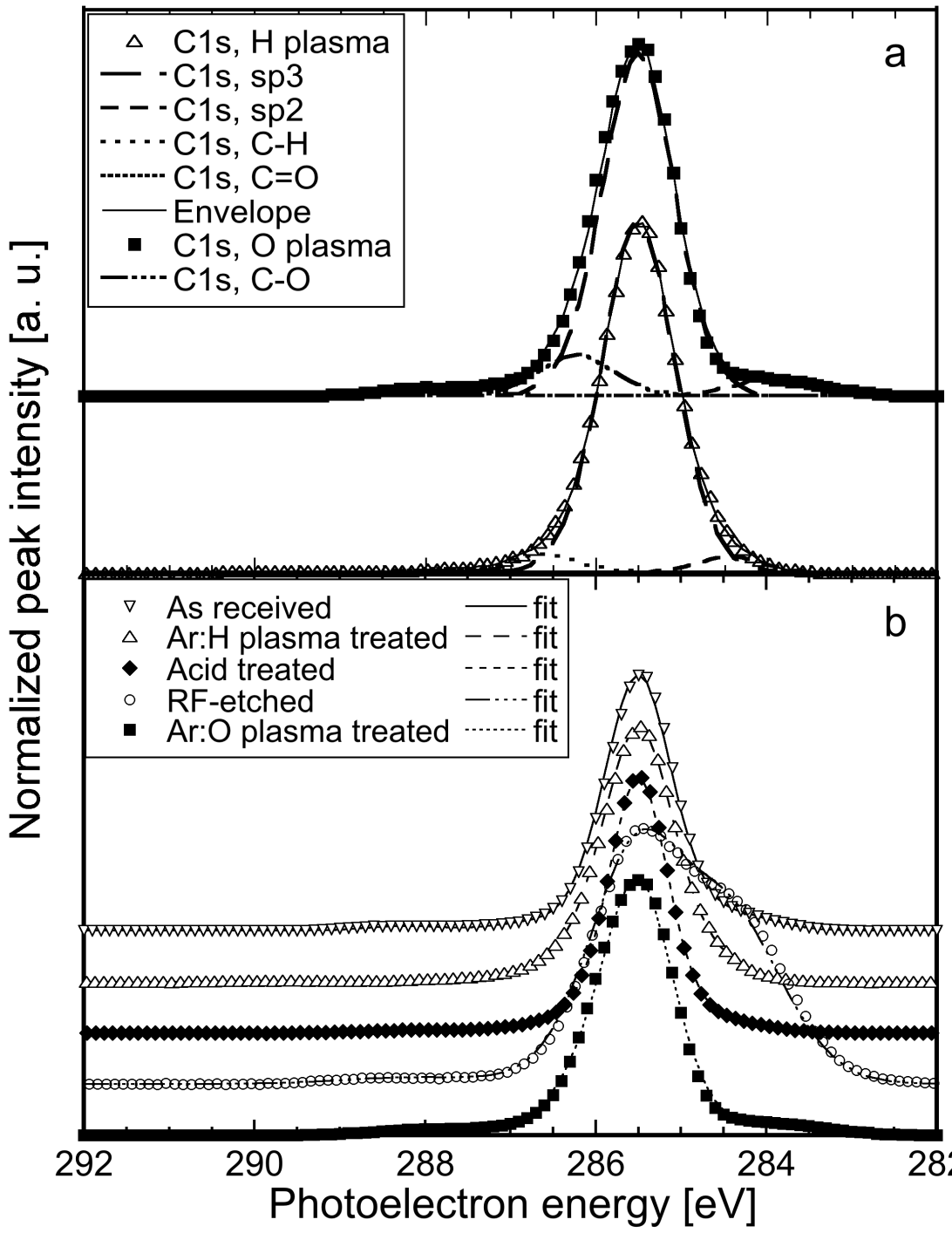

Figure 4. Recorded XPS signal around the C_s^1 peak of diamond as a function of sample surface treatment. (a) shows two examples of fitting using gaussian-lorentzian subpeaks for quantification and (b) shows the raw curves and their envelope fits.

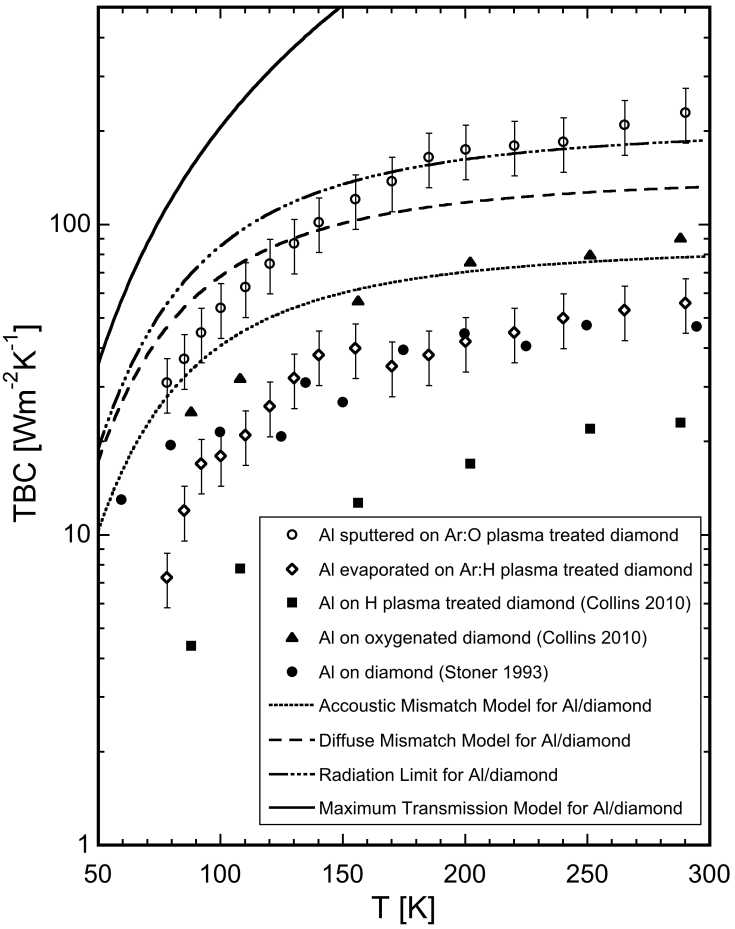

Figure 5. TBC results obtained for Ar:O (circles) and Ar:H (diamonds) plasma-treated samples with aluminum. Data from Stoner and Maris[29] (filled circles) and Collins *et al.*[9] (filled triangles: oxygenated, filled squares: hydrogenated) are shown for comparison. The curves show simple limits and models for Al/diamond TBC: radiation limit (dash-dotted curve), Diffuse Mismatch (dashed curve) and Acoustic Mismatch (dotted curve). Another limit called Maximum Transmission Model (not discussed in the text, see[33]) that takes inelastic interactions into account is put in plain curve as the maximum value that can be expected. The parameters used for the curves are: $\theta_{D,Al}$=425 K, $\theta_{D,C}$=2240 K, $v_{l,Al}$=6240 ms^{-1}, $v_{t,Al}$=3040 ms^{-1}, $v_{l,C}$=17500 ms^{-1}, $v_{t,C}$=12800 ms^{-1}.